Threonine 201 in the Diiron Enzyme Toluene 4-Monooxygenase Is Not Required for Catalysis†

Jeremie D. Pikus,‡ Kevin H. Mitchell,‡ Joey M. Studts,‡ Kevin McClay,§ Robert J. Steffan,§ and Brian G. Fox*,‡

The Institute for Enzyme Research, Graduate School, and Department of Biochemistry, College of Agricultural and Life Sciences, University of Wisconsin, Madison, Wisconsin 53705, and Envirogen, Inc., Lawrenceville, New Jersey 08648

Received September 21, 1999; Revised Manuscript Received November 8, 1999

ABSTRACT: The diiron enzyme toluene 4-monooxygenase from *Pseudomonas mendocina* KR1 catalyzes the NADH- and O_2-dependent hydroxylation of toluene. A combination of sequence alignments and spectroscopic studies indicate that T4MO has an active site structure closely related to the crystallographically characterized methane monooxygenase hydroxylase. In the methane monooxygenase hydroxylase, active site residue T213 has been proposed to participate in O_2 activation by analogy to certain proposals made for cytochrome P450. In this work, mutagenesis of the comparable residue in the toluene 4-monooxygenase hydroxylase, T201, has been used to investigate the role of an active site hydroxyl group in catalysis. Five isoforms (T201S, T201A, T201G, T201F, and T201K) that retain catalytic activity based on an in vivo indigo formation assay were identified, and detailed characterizations of the purified T201S, T201A, and T201G variants are reported. These isoforms have k_{cat} values of 1.2, 1.0, and 0.6 s^{-1}, respectively, and k_{cat}/K_M values that vary by only approximately 4-fold relative to that of the native isoform. Moreover, these isoforms exhibit 80−90% coupling efficiency, which also compares favorably to the >94% coupling efficiency determined for the native isoform. For the T201S, T201A, and T201G isoforms, the regiospecificity of toluene hydroxylation was nearly identical to that of the natural isoform, with *p*-cresol representing 90−95% of the total product distribution. In contrast, the T201F isoform caused a substantial shift in the product distribution, and gave *o*- and *p*-cresol in a 1:1 ratio. In addition, the amount of benzyl alcohol was increased ∼10-fold with the T201F isoform. For reaction with *p*-xylene, previous studies have shown that the native isoform reacted to give 4-methybenzyl alcohol and 2,5-dimethylphenol in a 4:1 ratio [Pikus, J. D., Studts, J. M., McClay, K., Steffan, R. J., and Fox, B. G. (1997) *Biochemistry 36*, 9283−9289]. For comparison, the T201S, T201A, and T201F isoforms gave a slightly relaxed 3:1 ratio of these products, while the T201G isoform gave a dramatically relaxed 1:1 ratio. On the basis of these studies, we conclude that the hydroxyl group of T201 is not essential to maintaining the turnover rate or the coupling of the toluene 4-monooxygenase complex. However, changing the volume occupied by the side chain at the position of T201 can lead to alterations in the regiospecificity of the hydroxylation, presumably by producing different orientations for substrate binding during catalysis.

The mechanisms by which heme and non-heme monooxygenases activate dioxygen for hydrocarbon oxidation has aroused considerable interest (*1*), and the identification of the chemical functional groups that facilitate O−O bond scission has been a topic of particular interest in recent years. Sequence alignments of the class I (bacterial/mitochondrial) and class II (microsomal) cytochrome P450[1] monooxygenases (*2*) reveal an almost universally conserved pairing of Asp or Glu with an adjacent Thr, while crystal structures (*3*−*7*) show that these residues are located in the active site. In the P450cam−CO−camphor ternary complex (*5*), the oxygen atom of CO is 4.4 Å away from the side chain oxygen of T252 (Figure 1A). Thus, the conserved Thr is positioned to have a role in catalysis, potentially as a proton donor to a heme-bound peroxo intermediate.

The role of the conserved Thr in P450 catalysis has been thoroughly investigated by mutagenesis. In P450cam and P450bm-3, mutation of the conserved Thr to Ala severely impaired hydroxylation due to an uncoupling of NADH consumption and substrate hydroxylation (*8*−*10*), while introduction of the same mutation in microsomal P450d and neuronal nitric oxide synthase resulted in increased catalytic activity and an increased level of coupling (*11*, *12*). Mutation of the conserved Thr to Ser generally resulted in only a slight

† This work was supported by the National Science Foundation Early Career Development Program (MCB-9733374) and the Petroleum Research Foundation (32955-AC4) through grants to B.G.F. and the National Science Foundation Small Business Innovation Research Program (DMI-9460076) through a grant to R.J.S. B.G.F. is a Shaw Scientist of the Milwaukee Foundation (1994−1999). K.H.M. is a trainee supported by NIH Institutional Biotechnology Pre-Doctoral Training Grant T32 GM08349.

* To whom correspondence should be addressed. E-mail: fox@enzyme.wisc.edu. Telephone: (608) 262-9708. Fax: (608) 265-2904.

‡ University of Wisconsin.

§ Envirogen, Inc.

[1] Abbreviations: compound P, peroxodiiron(III) intermediate of methane monooxygenase; compound Q, diiron(IV) intermediate of methane monooxygenase; MMOH, hydroxylase component of methane monooxygenase; P450, cytochrome P450 monooxygenase; T4MO, four-protein toluene 4-monooxygenase complex from *Pseudomonas mendocina* KR1; T4MOH, hydroxylase component of T4MO.

10.1021/bi992187g CCC: $19.00 © 2000 American Chemical Society
Published on Web 01/04/2000

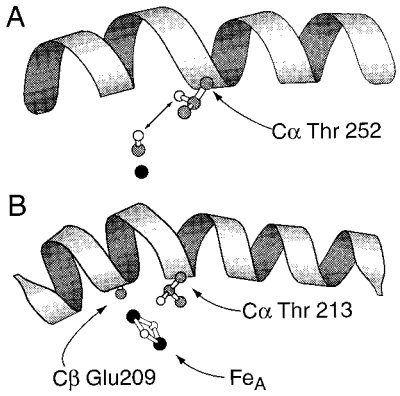

FIGURE 1: Location of active site Thr residues in two structurally distinct monooxygenases. Solid black spheres are iron atoms; gray spheres are carbon atoms, and white spheres are oxygen atoms. (A) Cytochrome P450cam−CO−camphor ternary complex (*5*). The double arrowhead line indicates the 4.4 Å separation of Oγ of T252 and the O atom of iron-bound CO. (B) Methane monooxygenase hydroxylase (*19*, *20*).

decrease in the level of coupling (*8*, *13*−*15*), suggesting that conservation of a side chain hydroxyl group at this position was sufficient for maintaining enzyme activity. However, when T252 in P450cam was mutated to methyl-O-Thr, the mutated isoform retained activity and was 100% coupled (*16*).[2] Furthermore, in some P450s, mutation of the conserved Thr alters the regiospecificity (*11*, *14*, *18*). Thus, there is considerable variability regarding the potential contributions of this residue in P450 catalysis.

While considerable experimental detail is available on the role of active site residues in the P450 monooxygenases, less is known about the role of active site residues in the diiron monooxygenases. X-ray structures show that MMOH T213 (Figure 1B) resides in a long α-helix with Oγ positioned 6.3 Å from Fe$_A$ and 6.8 Å from Fe$_B$ (*19*, *20*); Oγ is involved in an H-bond network with the active site water and one of the diiron-bridging oxygen atoms (*19*). Primary sequence alignments show that all diiron monooxygenases (*21*−*23*) have a Thr comparable to MMOH T213. This conserved Thr is located four residues after a conserved Glu that acts as a ligand to the diiron center (Table 1, E helix). Thus, the conserved Thr residues in the diiron monooxygenases are likely to occupy similar positions in the active site with respect to the diiron center. The acyl-ACP desaturases also have a comparable active site Thr residue (*21*, *24*) whose role in catalysis has not been reported. In contrast, ribonucleotide reductase has a Phe residue (F208 in the *Escherichia coli* enzyme) in a position comparable to that of the above-mentioned Thr (*25*). The proximity of this amino acid position to catalytic intermediates has been revealed by mutagenesis of this Phe residue to Tyr, which leads to a hydroxylation where the transferred O atom is derived from water (*26*, *27*), and by reaction of the doubly mutated isoform W48F/F208Y, which leads to a hydroxylation where the transferred O atom is derived from O_2 (*28*).

As discussed for the P450 family, the H-bonding interactions observed in the MMOH crystal structures and the sequence conservation observed in the other diiron monooxygenases and desaturases suggest that a Thr residue may have an important role in catalysis, possibly by acting as a proton donor during the O_2 activation steps of the reaction cycle (*19*, *21*). In this work, we report mutagenesis of T201, the putative active site Thr residue in T4MOH from *Pseudomonas mendocina* KR1, and the resultant effects on the catalytic activity, coupling efficiency, and product regiospecificity. In summary, the hydroxyl group of T201 is not essential to maintaining any of these three critical aspects during the toluene hydroxylation reaction.

MATERIALS AND METHODS

Materials. Vent DNA polymerase and all restriction enzymes were purchased from New England Biolabs (Beverly, MA). Wizard DNA preparation kits were from Promega (Madison, WI). DNA extraction and purification kits were from BIO101 (Vista, CA) and Qiagen (Valencia, CA), respectively. Toluene, *p*-xylene, *o*-, *m*-, and *p*-cresols, 4-methylbenzyl alcohol, 2,5-dimethylphenol, and all other chemicals were from Aldrich (Milwaukee, WI). *E. coli* strains DH5α (Pharmacia, Piscataway, NJ) and BL21(DE3) (Novagen, Madison, WI) were used for cloning and screening, and expression, respectively. PCR primers were purchased from Integrated DNA Technologies, Inc. (Coralville, IA).

Creation of T201A and T201S Isoforms. All PCRs were performed with Vent DNA polymerase and a model 9600 thermocycler (Perkin-Elmer, Foster City, CA). The primers used for mutagenesis are shown in Table 2. pRS204 (*29*) was used as the template for mutagenesis. Primers T201A5 and T2013 were used to make the T201A isoform; primers T201S5 and T2013 were used to make the T201S isoform. A PCR with 30 cycles of melting at 95 °C for 60 s, annealing at 55 °C for 30 s, and extending at 72 °C for 23 s was used to amplify a 364 bp fragment containing the respective T201A or T201S sequences. PCR-amplified products were gel-purified, digested with *Bst*BI and *Bgl*II, ligated with similarly digested pRS204, transformed into *E. coli* DH5α, and plated onto Luria-Bertani plates containing 100 μg/mL ampicillin. Plasmid DNA was isolated from the resultant transformants and was screened by digestion with *Stu*I to verify the presence of the desired sequence. Plasmid DNA containing the correct restriction pattern was then digested with *Eco*RI and *Bgl*II, and the resulting 962 bp fragment was gel-purified, ligated with similarly digested pKM10,[3] and transformed into *E. coli* BL21(DE3). DNA was isolated from the resultant transformants and sequenced using the Big Dye sequencing kit (Perkin-Elmer) at the University of Wisconsin Biotechnology Center to verify that the correct sequences were present. Plasmids containing the T201A and T201S isoforms were designated pJP20 and pJP21, respectively.

Saturation Mutagenesis. Saturation mutagenesis of T201 was accomplished through random oligonucleotide-mediated

[2] Hydroxylation of methyl-O-Thr could result in demethylation and restoration of active site Thr; O-demethylation is a well-characterized facet of P450 reactivity (*17*).

[3] The construction and characterization of pKM10 will be reported elsewhere (J. M. Studts, K. H. Mitchell, and B. G. Fox, unpublished results). This vector minimizes adventitious turnover of T4MOH [*tmoA*, *tmoB*, and *tmoE* gene products, $(\alpha\beta\gamma)_2$ quaternary structure with an M_r of ≈216 kDa] during heterologous expression because the Rieske ferredoxin (*tmoC* gene product), catalytic effector protein (*tmoD* gene product), and NADH oxidoreductase (*tmoF* gene product) required for electron transfer to T4MOH are not present.

Table 1: Active Site Residues in Methane Monooxygenase and Comparable Residues for Toluene Monooxygenases, Phenol Hydroxylase, and Alkene Epoxidase

MMO[a,b]	MMO[a,c]	T4MO[d]	T3MO[e]	T2MO[f]	dmpN[g]	amoC[h]	proposed function[i]	ref
				Residues in the B Helix (8 residues)				
L110	L110	I100	I100	V106	V105	L091	T4MO enantioselectivity[5]	
E	E	A101	A	T	S	T		
V	V	V102	L	P	P	N		
G	G	G103	G	L	L	A	T4MO enantioselectivity[5]	
E	E	E104	E	E	E	E	Fe_A ligand	*19*, *20*
Y	Y	Y105	Y	Y	Y	Y		
N	N	A106	A	A	Q	Q		
A	A	A107	A	A	A	A	T4MO enantioselectivity[5]	
				Residues in the C Helix (9 residues)				
D143	D143	D133	D133	D133	D133	D133	H-bond to the Fe_B His ligand	*19*, *20*
E	E	E134	E	E	E	E	Fe_A ligand	*19*, *20*
I	I	L135	N	L	L	V		
R	R	R136	R	R	R	R	H-bond to the F helix	
H	H	H137	H	H	H	H	Fe_A ligand	*19*, *20*
T	T	G138	G	Y	V	A		
H	H	Q139	Q	Q	Q	Q		
Q	Q	L140	L	T	T	L		
C	C	Q141	Q	E	Q	E	T4MO regioselectivity	*32*
				Residues in the D Helix (5 residues)				
F188	F188	F176	F176	F181	M180	F169	hydrophobic surface	*19*, *20*
S	A	D177	D	E	D	Q		
D	D	D178	D	D	D	H		
G	G	L179	L	A	A	F		
F	F	I180	F	C	R	N	hydrophobic surface	*32*
				Residues in the E Helix (14 residues)				
L204	L204	L192	L192	V196	V195	L184	hydrophobic surface	
Q	Q	T193	T	S	S	N		
L	L	F194	F	F	F	I		
V	V	S195	A	S	S	V		
G	G	F196	F	F	F	A	hydrophobic surface	
E	E	E197	E	E	E	E	Fe_B ligand	*19*, *20*
A	A	T198	T	Y	Y	T		
C	C	G199	G	V	V	A		
F	F	F200	F	L	L	F		
T	T	T201	T	T	T	T		this work
N	N	N202	N	N	N	N		
P	P	M203	M	L	L	I		
L	L	Q204	Q	L	L	L		
I	I	F205	F	F	F	L	T4MO regioselectivity	*32*
				Residues in the F Helix (15 residues)				
F236	F236	I224	I224	G228	G227	F216	hydrophobic surface	*19*, *20*
L	L	S225	S	F	F	L		
S	S	S226	S	S	S	S		
I	V	I227	I	A	A	I	hydrophobic surface	*19*, *20*
E	E	Q228	Q	Q	Q	Q		
T	T	T229	T	S	S	S		
D	D	D230	D	D	D	D	H-bond to the Fe_A His ligand	*19*, *20*
E	E	E231	E	E	E	E	Fe_B ligand	*19*, *20*
L	L	S232	S	S	A	A		
R	R	R233	R	R	R	R	H-bond to the C helix	
H	H	H234	H	H	H	H	Fe_B ligand	*19*, *20*
M	M	A235	A	M	M	M		
A	A	Q236	Q	T	T	A		
N	N	Q237	I	L	L	N		
G	G	G238	G	G	G	G		

[a] Fifty-one residues in five α-helices of MMOH identified by X-ray crystallography as forming the active site (*19*, *20*). Within each helical region, the residues that are shown are contiguous. Residues in naturally occurring toluene monooxygenases, phenol hydroxylase, and alkene epoxidase determined by alignment of primary sequences relative to conserved diiron center ligands. [b] MMOH from *Methylococcus capsulatus* (Bath) (Genbank accession no. M58499). [c] MMOH from *Methylosinus trichosporium* OB3b (Genbank accession no. X55394). [d] T4MOH from *Pseudomonas mendocina* KR1 (Genbank accession no. M65106). [e] T3MOH from *Ralstonia picketti* PKO1 (Genbank accession no. U04052). [f] T2MOH from *Pseudomonas* sp. strain JS150 (Genbank accession no. L40033). [g] Phenol hydroxylase from *Pseudomonas putida* sp. CF600 (Genbank accession no. M60276). [h] Alkene epoxidase from *Nocardia corallina* (Genbank accession no. D37875). [i] Proposed function for the residue in T4MOH based on site-directed mutagenesis studies of their effect on regiospecificity or enantioselectivity of the hydroxylation reactions (this work, ref *32*, and footnote 5).

overlap extension PCR (*30*). Figure 2 summarizes the locations of the primers on the *tmoA* gene and the order of steps used for saturation mutagenesis. Primers T201XF and T201XR (Table 2) were designed to exactly match the sequence of the *tmoA* gene except for the T201 codon. At the first base of the T201 codon, random nucleotides were

Table 2: Oligonucleotide Primers Used for Mutagenesis of Residue T201 in Toluene 4-Monooxygenase Hydroxylase

isoform	primer abbreviation	nucleotide sequence[a]
T201S	T201S5	cgttttcattcgaaaccggcttcaGcaacatgcagtttctAggCCtggcggcagatgc[b]
	T2013	ccagggcttgtccaagcccaga
T201A	T201A5	cgttttcattcgaaaccggcttcGccaacatgcagtttctAggCCtggcggcagatgc[b]
	T2013	ccagggcttgtccaagcccaga
T201X	T201XF	cggcttcNDBaacatgcagtttcttgggttggc
	T201XR	gccaacccaagaaactgcatgttBDNgaagccg
T201P	T201PF	ggcttcCCCaacatgcagtttcttgggttggc
	T201PR	gccaacccaagaaactgcatgttGGGgaagcc
	ABEF2	ccacaggcacggaattcaagaatatggcg
	BglIIR	cttgtccaagcccagatctatcaacgagcg

[a] The 5′-end of the oligonucleotide is at the left. N is a, t, g, or c. D is a, t, or g. B is t, g, or c. [b] Underlined sequences indicate position of a silent *Stu*I restriction site introduced for screening purposes.

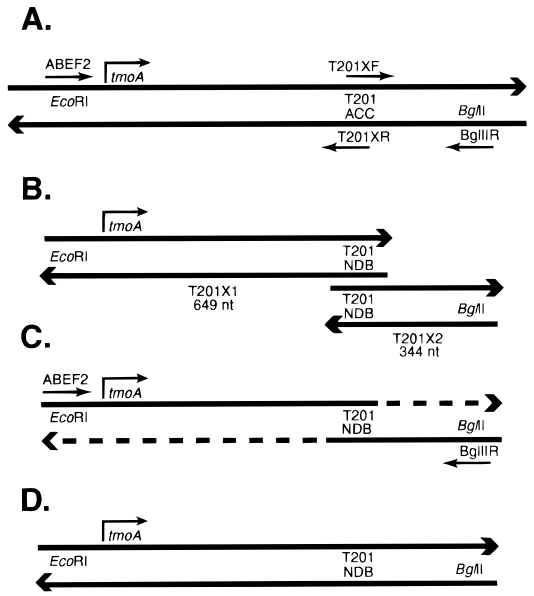

FIGURE 2: Summary of overlap extension PCR used to generate T201X isoforms of toluene 4-monooxygenase. The relative position of the *tmoA* start site is as indicated. (A) Location of forward and reverse primers used to generate fragments T201X1 (649 nucleotides) and T201X2 (344 nucleotides) overlapping at T201. (B) Purified DNA fragments T201X1 and T201X2 were used as the template for 10 rounds of primerless PCR. (C) After 10 rounds of primerless PCR, the outside primers ABEF2 and *Bgl*IIR were added to amplify the nascent 962 bp PCR product generated from the 10 rounds of primerless PCR. (D) Final 962 bp PCR product with the T201 codon randomized.

inserted during primer synthesis (N being a, t, g, or c). At the second base, cytosine was not permitted (D being a, t, or g), which eliminated Pro, Thr, and four of the six Ser codons from the pool of mutated isoforms. Consequently, a T201P isoform was generated independently by use of primers T201PF and T201PR and the steps outlined in Figure 2. At the third base, adenine was not permitted (B being t, g, or c), which eliminated the ochre (UAA) and opal (UGA) codons.

Overlap Extension PCR. Plasmid pKM10[3] was used as the PCR template. Primers ABEF2 and T201XR (Table 2) were used to generate fragment T201X1, while primers T201XF and *Bgl*IIR were used to generate fragment T201X2 (Table 2 and Figure 2). A PCR with 30 cycles of melting for 45 s at 94 °C, annealing for 30 s at 64 °C, and extending for 40 s at 72 °C was used. The amplified DNA fragments T201X1 and T201X2 were purified and then used as the template for primerless PCR. After 10 cycles of melting for 45 s at 94 °C, annealing for 45 s at 58 °C, and extending for 80 s at 72 °C, primers ABEF2 and *Bgl*IIR were added for an additional 20 cycles to enhance amplification of the complete 962 bp fragment.

T201X Library and Screen for Functional Isoforms. The 962 bp fragments containing the T201X mutations were purified, digested with restriction enzymes *Eco*RI and *Bgl*II, and repurified. For functional screening, the digested fragments were ligated into similarly digested pRS184f (*29*), transformed into *E. coli* BL21(DE3) (Novagen) by heat shock, and plated onto Luria-Bertani agar plates containing 100 μg/mL ampicillin. The resulting transformants were cultured on Luria-Bertani agar plates containing ampicillin (200 μg/mL) that had been top-spread with both indole (75 μL of a 100 mM solution in 50% ethanol) and IPTG (50 μL of a 100 mM solution in sterile deionized water). Transformants exhibiting color formation were isolated to single colonies, and the plasmids were then purified from the isolated colonies using the Wizard mini-prep kit. Mutations at residue T201 were identified using the Big Dye sequencing kit as described above.

Overexpression of T201 Isoforms. For overexpression, pRS184f containing the desired T201X mutation was digested to release either an *Msc*I−*Bgl*II fragment or an *Eco*RI−*Bgl*II fragment. The resultant 962 bp fragment was repurified and ligated into similarly digested pKM10.[3] The

pKM10-derived plasmids encoding the T201S, T201A, and T201G isoforms were transformed into *E. coli* BL21(DE3), and a single colony derived from the transformation was used to inoculate 2 mL of Luria-Bertani medium amended with 150 μg/mL ampicillin. This culture was grown to an optical density at 600 nm of ~0.1, and then 1 mL aliquots were used to inoculate two 500 mL cultures of Luria-Bertani medium containing 150 μg/mL ampicillin. The cultures were grown to an optical density at 600 nm of 0.5−1.0, and were then used to inoculate 10 L of Luria-Bertani medium in a New Brunswick Scientific BIOFLO 3000 fermenter. When the fermenter culture reached an optical density at 600 nm of ~3−4, protein expression was induced by the addition of 66 g of β-D-lactose and 22 mL of an iron-containing solution (1.12 g of $FeSO_4 \cdot 7H_2O$ dissolved in 95 mL of deionized water acidified with 5 mL of 0.25 M H_2SO_4). After 4 h, the cells were harvested by centrifugation (24000*g* for 10 min) and stored at −80 °C. Ten liters of culture medium yielded ~70 g of wet cell paste. For all isoforms, expression of T4MOH polypeptides was verified by analysis of whole cell lysates using denaturing gel electrophoresis (*31*).

The pKM10 plasmid containing the T201F isoform was transformed into *E. coli* BL21(DE3) cells, and a single colony was used to inoculate a 2 L Erlenmeyer flask containing 500 mL of Luria-Bertani medium and 300 μg/mL ampicillin. When the culture reached an optical density at 600 nm of 0.8−1.0, expression was induced by the addition of 4 g of β-D-lactose, 1 g of Casamino acids, and 2 mL of the iron-containing solution described above. After 4 h, the cells were harvested by centrifugation. Five hundred milliliters of culture medium yielded ~1.5 g of wet cell paste. The cell pellet was resuspended in 5 mL of 50 mM phosphate buffer (pH 7.5) and lysed by sonication. The cell debris was removed by centrifugation in a microcentrifuge (14 000 rpm for 10 min at 4 °C), and the cell-free supernatant was used for regiospecificity studies.

Enzyme Purification, Catalytic Characterizations, and Regiospecificity. The T201S, T201A, and T201G isoforms were overexpressed as described above, purified, and characterized for iron content (*29*), catalytic activity, coupling efficiency, and product regiospecificity (*29*, *32*).

Steady-state kinetic measurements were performed using a Clark-type electrode (Yellow Springs Instruments, Yellow Springs, OH) and custom-built amplifier (*33*) to monitor changes in the dissolved O_2 concentration. The polarograph sensitivity was calibrated to provide a full-scale response when 50 nmol of O_2 was consumed by purified 3,4-protocatechuate dioxygenase in the irreversible oxygenation of 50 nmol of recrystallized protocatechuic acid (*33*). The electrode chamber contained 50 mM phosphate buffer (pH 7.5), T4MOH (~0.4 nmol of diiron sites), Rieske ferredoxin (T4MOC, 0.4 nmol), catalytic effector protein (T4MOD, 0.9 nmol), and NADH oxidoreductase (T4MOF, 0.1 nmol) in a total volume of 1.7 mL. The electrode chamber was sealed with a ground glass stopper containing a narrow bore syringe port. Toluene (as an ethanolic solution) was added using a gastight Hamilton syringe to give an initial toluene concentration in the electrode chamber in the range of 2−100 μM. A stable baseline was established, and the reaction was initiated by the addition of NADH to an initial concentration of 500 μM. Dissolved O_2 was provided by using buffer equilibrated with air, and all reactions were performed at room temperature. Kinetic constants were determined by varying the toluene concentration, while the concentrations of all constituents of the enzyme complex, NADH, and O_2 were fixed at the initial values described above. Initial reaction velocities were determined as the rate of change in O_2 concentration over a 1−2 min time period after correction for baseline deflections. The steady-state kinetic parameters k_{cat} and apparent K_M were determined by nonlinear least-squares fitting of the initial reaction velocities, v, and the substrate concentrations, [S], to the Michaelis−Menten equation, $v = k_{cat}[S]/(K_M + [S])$. In this work, the turnover number, k_{cat}, is expressed relative to the diiron center concentration. Nonlinear least-squares fitting was performed using DeltaGraph Pro 3.0 (DeltaPoint, Monterey, CA).

Coupling efficiency studies were performed in a magnetically stirred 3 mL quartz cuvette containing 50 mM potassium phosphate buffer (pH 7.5), T4MOH (2 nmol), Rieske ferredoxin (T4MOC, 2 nmol), catalytic effector protein (T4MOD, 4 nmol), and NADH oxidoreductase (T4MOF, 0.4 nmol) in a total volume of 1.99 mL. The cuvette was sealed with a rubber septum, and then 1 μL of neat toluene was added to the buffer solution. The reaction was initiated by the addition of NADH (300 nmol in 10 μL of buffer), and the reaction was monitored by following the decrease in absorbance at 340 nm. When the NADH was depleted, an aliquot was extracted and analyzed for *p*-cresol content (*29*). Coupling efficiency was calculated as the fraction of the nanomoles of *p*-cresol produced relative to the nanomoles of NADH consumed.

Product distributions from the hydroxylation of toluene and *p*-xylene were determined by gas chromatography using a Hewlett-Packard 6890 gas chromatograph equipped with a 7683 auto injector and an EC-WAX column (30 m × 0.25 mm, 0.25 μm film thickness, Alltech Associates, Inc., Deerfield, IL) connected to a flame ionization detector. The injector and detector were maintained at 250 °C. The He carrier flow rate was 4.0 mL/min. For the separation of toluene oxidation products, the column temperature was initially held at 80 °C and increased to 140 °C at a rate of 5 °C/min. Under these conditions, the benzyl alcohol and *o*-, *p*-, and *m*-cresols eluted at 6.5, 8.5, 9.7, and 9.9 min, respectively. For the separation of *p*-xylene oxidation products, the column temperature was initially held at 100 °C for 1 min and then increased to 130 °C at a rate of 5 °C/min. Under these conditions, 4-methylbenzyl alcohol and 2,5-dimethylphenol eluted at 7.7 and 10.0 min, respectively. All retention times were verified using neat compounds.

RESULTS

Mutagenesis Results. Two strategies for mutagenizing the T201 codon in the *tmoA* gene were developed. Rational mutagenesis was used to introduce codons for Ser, Ala, and Pro at this position, while random mutagenesis via overlap extension PCR was used to saturate this position with codons for the other amino acids. For screening, plasmid pRS184f provides functional expression of the complete T4MO complex in *E. coli* (*29*). When grown in the presence of indole, *E. coli* transformants expressing functional T4MO hydroxylate indole at the 3-position, which ultimately yields the blue dye indigo (*34*−*36*). This visual screen was used

Table 3: Characterization of Catalytically Active Isoforms Recovered from Saturation Mutagenesis of T201 in Toluene 4-Monooxygenase

isoform[a]	yield[b] (mg)	iron content[c]	k_{cat} (s^{-1})[d]	K_M (μM)	k_{cat}/K_M (s^{-1} μM^{-1})	coupling[e] (%)
T201	22.6	2.2 (0.2)	1.3 (0.1)	5 (2)	0.3 (0.1)	94 (2)
T201S	20.4	2.0 (0.2)	1.2 (0.2)	6 (3)	0.2 (0.1)	88 (3)
T201A	19.2	1.9 (0.3)	1.0 (0.1)	6 (2)	0.17 (0.06)	90 (2)
T201G	18.0	2.6 (0.2)	0.6 (0.1)	9 (1)	0.07 (0.01)	81 (2)

[a] Isoforms T201F and T201K gave a faint response in the in vivo screening assay; the regioselectivity of T201F was investigated using cell-free extracts, while T201K was not further characterized due to low activity. The following isoforms were recovered from mutagenesis but did not exhibit catalytic activity for indole oxidations: T201C, T201D, T201H, T201I, T201L, T201M, T201N, T201P, T201Q, T201V, T201W, and T201Y. Isoforms T201E and T201R were not recovered from the screening process. [b] Milligrams of purified enzyme obtained per liter of culture medium. [c] Moles of Fe per mole of purified $\alpha\beta\gamma$ protomer. [d] Maximal turnover number relative to an $\alpha\beta\gamma$ protomer in reaction mixtures containing optimal concentrations of the other proteins of the T4MO complex, saturating NADH (0.5 mM), and saturating toluene (5.8 mM at 25 °C) in 50 mM phosphate buffer (pH 7.5) at 25 °C. [e] Ratio of NADH consumed vs hydroxylated products recovered from utilization of 300 nmol of NADH in the presence of optimal concentrations of the other proteins of the T4MO complex and saturating toluene.

to identify catalytically active mutated isoforms, and provided three new isoforms with catalytic activity: T201G, T201F, and T201K. Sequencing of plasmid DNA isolated from other noncolored transformants provided all other isoforms except T201E and T201R. Transformants containing the natural isoform and the mutated T201S, T201A, and T201G isoforms developed a more intense blue color than transformants containing either the T201F or T201K isoform, which only developed a pink to faint purple coloration. For this study, the apparently more active T201S, T201A, and T201G isoforms were overexpressed, purified, and more fully characterized. In addition, cell-free extracts were used to evaluate the regiospecificity of the T201F isoform.

Expression and Properties of Active T4MOH Isoforms. To enhance the expression of the various isoforms, the regions containing the respective mutations were cloned into pKM10.[3] Expression from this vector resulted in comparable levels of protein expression for each isoform as judged by SDS−PAGE. During purification of the T201S, T201A, and T201G isoforms, the chromatographic properties were indistinguishable from those of the natural isoform, and the purified yield of each was ~20 mg per liter of fermenter culture (Table 3). SDS−PAGE analysis revealed that each purified mutated isoform had the same pattern of subunit polypeptides (52, 38, and 9 kDa) present in the natural isoform. Iron analysis revealed that all purified isoforms contained ~2 mol of iron per diiron binding site (Table 3), suggesting that a full complement of diiron centers was present in each.

Catalytic Properties of Purified T4MOH Isoforms. Table 3 shows the catalytic activities and coupling efficiencies for the purified enzyme isoforms. Using the same preparations of the other T4MO components and the identical assay conditions, the natural isoform had a k_{cat} of 1.3 s^{-1} and exhibited a 94% coupling efficiency. Table 3 shows that the T201S, T201A, and T201G isoforms had turnover numbers of 1.2, 1.0, and 0.6 s^{-1}, respectively, while the coupling efficiency for all three isoforms was in the 80−90% range.

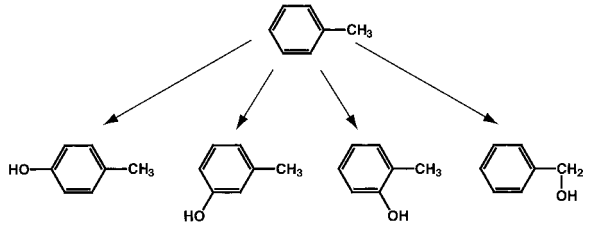

	A	B	C	D
T201	96.0	2.8	0.4	0.8
T201S	95.4	1.4	1.5	1.7
T201A	94.2	1.6	2.9	1.3
T201G	94.3	0.1	4.5	1.1
T201F	46.6	n.d.	41.9	11.5

FIGURE 3: Product distributions observed during the hydroxylation of toluene by the natural isoform and the mutated T201S, T201A, T201G, and T201F isoforms of recombinant toluene 4-monooxygenase. For all isoforms, purified enzyme reaction conditions were adjusted so that ≈300 nmol of total products was obtained. The product distributions were determined by averaging the results from three separate experiments using different preparations of the same isoform. The total deviation in product ratios was ≈2%; the minor products were reproducibly detected in all replicate assays. n.d., not detected.

Among these four variants, the selectivity parameter k_{cat}/K_M varied by only 4-fold for toluene oxidation, indicating that the catalytic properties of these different isoforms were affected only slightly by the presence of the different amino acids. As determined during this work by steady-state kinetic measurements using O_2 polarography, the natural isoform had an apparent K_M for toluene of 5 μM. This value is close to that estimated previously (*32*) by using gas chromatography, and is ~10^3-fold lower than the solubility limit for toluene at 25 °C. The mutated isoforms had similar apparent K_M values for toluene. Thus, the T201S and T201A isoforms had apparent K_M values of 6 μM, while the T201G isoform had a K_M value of 9 μM.

Regiospecificity of Toluene Hydroxylation. The regiospecificity for toluene oxidation is shown in Figure 3. The natural isoform exhibits a strong specificity for para hydroxylation of toluene, with *p*-cresol (96.0%), *m*-cresol (2.8%), *o*-cresol (0.4%), and benzyl alcohol (0.8%) representing the product distribution (*32*). Hydroxylation of toluene by the T201S, T201A, and T201G isoforms did not result in a substantial deviation from the product distributions of the natural isoform. For these three isoforms, T201G gave the largest shift for any single product, and yielded 4.5% *o*-cresol. In contrast, T201F gave a large redistribution of toluene oxidation products, and yielded nearly equal proportions of *o*- and *p*-cresol (41.9 and 46.6%, respectively). Notably, the T201F isoform also provided the only substantial shift in selectivity toward benzyl alcohol formation (11.5%).

Regiospecificity of p-Xylene Hydroxylation. *p*-Xylene is a useful alternative substrate for the study of T4MOH catalysis because only two hydroxylation products are possible. Furthermore, these two products are derived from either aromatic or benzylic hydroxylation, which may potentially arise from different mechanisms of oxidation (*17*). Figure 4 shows the regiospecificity for *p*-xylene hydroxylation by the various T201 isoforms. Previous studies showed that the natural isoform yielded 82% 4-methylbenzyl alcohol and 18% 2,5-dimethylphenol (*32*). As observed for toluene oxidation, the T201S and T201A isoforms had regiospecificities similar to the natural isoform, and yielded ~75% 4-methylbenzyl alcohol and ~25% 2,5-dimethylphenol.

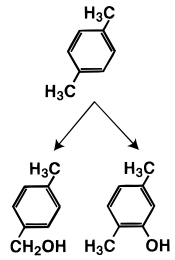

	A	B
T201	82.0	18.0
T201S	74.2	25.8
T201A	75.7	24.3
T201G	49.1	50.9
T201F	73.7	26.3

FIGURE 4: Product distributions observed during the oxidation of *p*-xylene by the natural isoform and the mutated T201S, T201A, T201G, and T201F isoforms of recombinant toluene 4-monooxygenase. Reaction conditions were as described in the legend of Figure 3.

Furthermore, the T201F isoform also gave a product distribution for *p*-xylene oxidation similar to that of the natural isoform, which is unlike the divergent results observed for toluene oxidation by the natural and T201F isoforms (Figure 3). For the T201G isoform, the regiospecificity of *p*-xylene oxidation was substantially different from that of the natural isoform, as 4-methylbenzyl alcohol and 2,5-dimethylphenol were produced in nearly equal proportions.

DISCUSSION

Among the diiron enzymes, recombinant forms of crystallographically characterized ribonucleotide reductase R2 (*26*−*28*, *37*−*42*) and stearoyl-ACP Δ^9 desaturase (*43*) have been subjected to functional analysis using mutagenesis methods. Intensive efforts to apply these methods to the study of MMOH have not been abundantly successful (*44*).[4] In contrast, T4MO has been amenable to heterologous expression (*29*, *35*, *36*, *45*, *46*) and mutagenesis (*32*, *46*)[5] and thus provides an opportunity to further examine structure−function relationships in the diiron hydroxylase class.

Mutagenesis of T4MOH. In this work, both rational and random mutagenesis approaches were applied in studying T201 in T4MOH. Initially, T201S and T201A were produced by rational mutagenesis and found to be catalytically active. Subsequently, random mutagenesis was used to assemble a T201X library consisting of all of the other amino acids except T201P, which was produced by rational mutagenesis and found to be catalytically inactive. The initial selection for active isoforms from the T201X library was based on the T4MOH-catalyzed oxidation of indole leading to indigo formation (*35*). Using this screen, 18 out of 20 possible amino acid substitutions at T201 were sorted into either functional or nonfunctional classes (Table 3). For all of the active isoforms identified by the appearance of colored products derived from indole hydroxylation, the ability to oxidize toluene was also retained. Whether the isoforms presently assigned to be inactive are actually expressed in a soluble form, incorporate a diiron center, or have catalytic activities other than indole hydroxylation remains to be determined.

Models of Proton Delivery in P450. There are numerous proposals for how the protons necessary for heterolytic O−O bond scission are delivered during the P450 reaction. Unlike the heme peroxidases, which have a catalytic His for this purpose (*47*), P450s have no obvious catalytic acidic or basic group(s) in the active site. Thus, most proposals involve transmission of protons through a network of H-bonded water molecules and amino acid residues connecting the active site to bulk solvent. One such model is the distal charge relay system proposed for P450cam (*48*−*50*), in which the side chain hydroxyl group of T252 is part of an H-bond network, including active site water molecules, conserved D251, and positively charged surface residues. Several other models for proton transfer have also been proposed for P450cam (*51*, *52*), including the participation of a backbone carbonyl and ordered water molecules in the distal helix groove for P450bm-3 and P450terp (*53*). Moreover, in the case of P450eryf, which does not have an active site Thr residue, a substrate-assisted water molecule and an associated H-bond network have been proposed to protonate the peroxo intermediate (*54*). Thus, it has been suggested that the nature of the proton donor depends on the enzyme isoform being studied, and that a single proton delivery model may not be applicable to all P450s (*53*).

Position of T201 with Respect to the T4MOH Diiron Center. Table 1 correlates the identity and spacing of iron ligands and other residues found in the MMOH active site with the comparable residues determined by alignment of the primary sequences of naturally occurring toluene monooxygenases, phenol hydroxylase, and alkene epoxidase. In each of these diiron hydroxylases, a Thr is located four residues after an essential iron ligand Glu (Figure 1B). Thus, assuming that the π-bend of the E helix is also conserved in the diiron monooxygenase family, it is likely that Thr will occupy the same position relative to the diiron center in all of these enzymes.

Role of T201 in T4MOH Catalysis. Given the variety of proposals for proton delivery that are available for P450s, it has also been of interest to determine whether and when proton delivery is required in the functionally analogous diiron monooxygenases. The recent studies of Lee and Lipscomb on MMOH from *Methylosinus trichosporium* OB3b have revealed the requirements for a single proton transfer in both the formation and the decay of compound P and the requirement for a single proton in the formation of compound Q (*55*). This work is the first direct demonstration of proton transfers in the O_2 activation steps of a diiron hydroxylase.

The crystal structures of MMOH (*19*, *20*) reveal the presence of an H-bonded network that includes Oγ of T213, a water bridge of the diiron cluster, and other active site water molecules (*19*). One possible function of Oγ in this H-bonding network may be to transfer protons within the active site during catalysis. However, the values for k_{cat}, k_{cat}/K_M, and coupling efficiency presented here (Table 3) show that the hydroxyl group of T201 is not essential for T4MOH catalysis.[6] This conclusion is in accord with those made in the *M. trichosporium* OB3b MMOH study (*55*), where a combination of the pK_a value of 7.6 and the linear proton

[4] M. DeFlaun, B. G. Fox, K. McClay, and R. J. Steffan, unpublished results.

[5] K. McClay, J. M. Studts, B. G. Fox, and R. J. Steffan, manuscript in preparation.

inventory plot are inconsistent with Thr acting as the singular, intimate proton donor. Instead, Lee and Lipscomb postulate that the proton donor in the MMOH reaction will be an iron-bound water molecule, and that Thr may act as an H-bond acceptor to help stabilize the peroxy-level intermediate. If this scenario is also at play in T4MOH, an active site water molecule could conceivably take the place of T201 Oγ in the T201A and T201G isoforms, thus resulting in the observed minor perturbations of catalytic properties. A determination of whether the larger side chain present in the T201F isoform is capable of excluding this putative active site water is beyond the scope of this study.

Contribution of T201 to T4MOH Regiospecificity. Table 1 shows the residues of T4MO (investigated here) that contribute to the regiospecificity of toluene, *m*-xylene, and *p*-xylene hydroxylation (*32*) or to the enantiomeric excess of butadiene epoxidation.[5] With the exception of T201F, the T201 isoforms that are studied here exhibit regiospecificities for hydroxylation of toluene that are nearly identical to that observed for the natural isoform, indicating that T201 does not provide significant contributions to the orientation of binding for the natural substrate. Furthermore, while the T201F isoform does not appear to fill the active site enough to occlude substrate binding, the addition of the more bulky phenyl group clearly affects the orientation of toluene within the active site. For oxidation of the larger substrate *p*-xylene, substitution of the smallest residue Gly for Thr caused substantial alterations in the product distribution obtained from *p*-xylene (Figure 4), while the Ser, Ala, and Phe substitutions had relatively minor effects on the product distribution. These results show that introduction of a different residue at the position of T201 can produce changes in active site volume that are both accessible to substrate and that can permit a changed orientation of binding relative to the diiron oxidant. These results extend our previous mapping of residues contributing to the regiospecificity of T4MOH catalysis (*32*).

CONCLUSIONS

The studies presented here reveal that T201 of T4MO, which has an identically conserved counterpart in all published sequences of diiron monooxygenases (and also in all sequences of acyl-ACP desaturases), is not essential for proton delivery during T4MO catalysis. Given the relative insensitivity of the kinetic parameters and coupling percentages to changes between Thr, Ser, Ala, and Gly at this position, the origin of the conservation of this amino acid in an otherwise well-diverged catalytic family of enzymes is now unclear. The combination of randomized mutagenesis, in vivo selections, and diagnostic catalytic characterizations used here represents a promising pathway for further elucidation of this evolutionary problem and other site-specific contributions of amino acids in the diiron monooxygenases.

[6] The possibility exists that product release may be strongly rate-limiting for the toluene 4-monooxygenase reaction. This would tend to mask any deleterious effects on k_{cat} resulting from this mutagenesis. However, the coupling of NADH consumption and product formation in the mutated isoforms remained high (~90%), which also seems inconsistent with an absolute requirement for HOγ of T201 in the catalytic reaction.

REFERENCES

1. Holm, R. H., and Solomon, E. I. (1996) *Chem. Rev. 96*, 2237−3042.
2. Nebert, D. W., and Nelson, D. R. (1991) *Methods Enzymol. 206*, 3−11.
3. Poulos, T. L. (1986) in *Cytochrome P-450: Structure, Mechanism, and Biochemistry* (Ortiz de Montellano, P. R., Ed.) pp 505−524, Plenum Press, New York.
4. Poulos, T. J., and Ragg, R. (1992) *FASEB J. 6*, 674−679.
5. Raag, R., and Poulos, T. L. (1989) *Biochemistry 28*, 7586−7592.
6. Hasemann, C. A., Ravichandran, K. G., Peterson, J. A., and Deisenhofer, J. (1994) *J. Mol. Biol. 236*, 1169−1185.
7. Ravichandran, K. G., Boddupalli, S. S., Hasermann, C. A., Peterson, J. A., and Deisenhofer, J. (1993) *Science 261*, 731−736.
8. Imai, M., Shimada, H., Watanabe, Y., Matsushima-Hibiya, Y., Makino, R., Koga, H., Horiuchi, T., and Ishimura, Y. (1989) *Proc. Natl. Acad. Sci. U.S.A. 86*, 7823−7827.
9. Martinis, S. A., Atkins, W. A., Stayton, P. S., and Sligar, S. G. (1989) *J. Am. Chem. Soc. 111*, 9252−9253.
10. Yeom, H., Sligar, S. G., Li, H., Poulos, T. L., and Fulco, A. (1995) *Biochemistry 34*, 14733−14740.
11. Furuya, H., Shimizu, T., Hirano, K., Hatano, M., and Fujii-Kuriyama, Y. (1989) *Biochemistry 28*, 6848−6857.
12. Sagami, I., and Shimizu, T. (1998) *J. Biol. Chem. 273*, 2105−2108.
13. Chen, S., and Zhou, D. (1992) *J. Biol. Chem. 267*, 22587−22594.
14. Fukuda, T., Imai, Y., Komori, M., Nakamura, M., Kusunose, E., Satouchi, K., and Kusunose, M. (1993) *J. Biochem. (Tokyo) 113*, 7−12.
15. Hanioka, N., Gonzalez, F. J., Lindberg, N. A., Liu, G., Gelboin, H. V., and Korzekwa, K. R. (1992) *Biochemistry 31*, 3364−3370.
16. Kimata, Y., Shimada, H., Hirose, T., and Ishimura, Y. (1995) *Biochem. Biophys. Res. Commun. 208*, 96−102.
17. Sono, M., Roach, M. P., Coulter, E. D., and Dawson, J. H. (1996) *Chem. Rev. 96*, 2841−2887.
18. Imai, Y., and Nakamura, M. (1989) *Biochem. Biophys. Res. Commun. 158*, 717−722.
19. Rosenzweig, A. C., Nordlund, P., Takahara, P. M., Frederick, C. A., and Lippard, S. J. (1995) *Chem. Biol. 2*, 409−418.
20. Elango, N., Radhakrishnan, R., Froland, W. A., Wallar, B. J., Earhart, C. A., Lipscomb, J. D., and Ohlendorf, D. H. (1997) *Protein Sci. 6*, 556−568.
21. Fox, B. G., Shanklin, J., Ai, J., Loehr, T. M., and Sanders-Loehr, J. (1994) *Biochemistry 33*, 12776−12786.
22. Byrne, A. M., Kukor, J. J., and Olsen, R. H. (1995) *Gene 154*, 65−70.
23. Johnson, G. R., and Olsen, R. H. (1995) *Appl. Environ. Microbiol. 61*, 3336−3346.
24. Lindqvist, Y., Huang, W., Schneider, G., and Shanklin, J. (1996) *EMBO J. 15*, 4081−4092.
25. Nordlund, P., and Eklund, H. (1993) *J. Mol. Biol. 232*, 123−164.
26. Ormö, M., deMaré, F., Regnström, K., Åberg, A., Sahlin, M., Ling, J., Loehr, T. M., Sanders-Loehr, J., and Sjöberg, B.-M. (1992) *J. Biol. Chem. 267*, 8711−8714.
27. Åberg, A., Ormö, M., Nordlund, P., and Sjöberg, B.-M. (1993) *Biochemistry 32*, 9845−9850.
28. Parkin, S. E., Chen, S., Ley, B. A., Mangravite, L., Edmondson, D. E., Huynh, B. H., and Bollinger, J. M., Jr. (1998) *Biochemistry 37*, 1124−1130.
29. Pikus, J. D., Studts, J. M., Achim, C., Kauffmann, K. E., Münck, E., Steffan, R. J., McClay, K., and Fox, B. G. (1996) *Biochemistry 35*, 9106−9119.
30. Ho, S. N., Hunt, H. D., Horton, R. M., Pullen, J. K., and Pease, L. R. (1989) *Gene 77*, 51−59.
31. Schägger, H., and von Jagow, G. (1987) *Anal. Biochem. 166*, 368−379.
32. Pikus, J. D., Studts, J. M., McClay, K., Steffan, R. J., and Fox, B. G. (1997) *Biochemistry 36*, 9283−9289.

33. Whittaker, J. W., Orville, A. M., and Lipscomb, J. D. (1990) *Methods Enzymol. 188*, 82−88.
34. Ensley, B. D., Ratzkin, B. J., Osslund, T. D., Simon, M. J., Wackett, L. P., and Gibson, D. T. (1983) *Science 222*, 167−169.
35. Winter, R. B., Yen, K. M., and Ensley, B. D. (1989) *Bio/Technology 7*, 282−285.
36. Yen, K.-M., Karl, M. R., Blatt, L. M., Simon, M. J., Winter, R. B., Fausset, P. R., Lu, H. S., Harcourt, A. A., and Chen, K. K. (1991) *J. Bacteriol. 173*, 5315−5327.
37. Bollinger, J. M., Jr., Krebs, C., Vicol, A., Chen, S., Ley, B. A., Edmondson, D. E., and Huynh, B. H. (1998) *J. Am. Chem. Soc. 120*, 1094−1095.
38. Larsson, Å., Climent, I., Nordlund, P., Sahlin, M., and Sjöberg, B.-M. (1996) *Eur. J. Biochem. 237*, 58−63.
39. Ormö, M., Renström, K., Wang, Z., Que, L., Jr., Sahlin, M., and Sjöberg, B.-M. (1995) *J. Biol. Chem. 270*, 6570−6576.
40. Regnström, K., Åberg, A., Ormö, M., Sahlin, M., and Sjöberg, B.-M. (1994) *J. Biol. Chem. 269*, 6355−6361.
41. Sahlin, M., Lassmann, G., Pötsch, S., Slaby, A., Sjöberg, B.-M., and Gräslund, A. (1994) *J. Biol. Chem. 269*, 11699−11702.
42. Climent, I., Sjöberg, B.-M., and Huang, C. Y. (1992) *Biochemistry 31*, 4801−4807.
43. Cahoon, E. B., Lindqvist, Y., Schneider, G., and Shanklin, J. (1997) *Proc. Natl. Acad. Sci. U.S.A. 94*, 4872−4877.
44. Jahng, D., and Wood, T. K. (1994) *Appl. Environ. Microbiol. 60*, 2473−2482.
45. Yen, K.-M., and Karl, M. R. (1992) *J. Bacteriol. 174*, 7253−7261.
46. McClay, K., Fox, B. G., and Steffan, R. J. (1996) *Appl. Environ. Microbiol. 62*, 2716−2722.
47. Poulos, T. L., and Kraut, J. (1980) *J. Biol. Chem. 255*, 8199−8205.
48. Gerber, N. C., and Sligar, S. G. (1992) *J. Am. Chem. Soc. 114*, 8742−8743.
49. Gerber, N. C., and Sligar, S. G. (1994) *J. Biol. Chem. 269*, 4260−4266.
50. Vidakovic, M., Sligar, S. G., Li, H., and Poulos, T. L. (1998) *Biochemistry 37*, 9211−9219.
51. Harris, D., and Loew, G. (1996) *J. Am. Chem. Soc. 118*, 6377−6387.
52. Oprea, T. I., Hummer, G., and Garcia, A. E. (1997) *Proc. Natl. Acad. Sci. U.S.A. 94*, 2133−2138.
53. Hasemann, C. A., Kurumbail, R. G., Boddupalli, S. S., Peterson, J. A., and Deisenhofer, J. (1995) *Structure 15*, 41−62.
54. Cupp-Vickery, J. R., Han, O., Hutchinson, C. R., and Poulos, T. L. (1996) *Nat. Struct. Biol. 3*, 632−637.
55. Lee, S.-K., and Lipscomb, J. D. (1999) *Biochemistry 38*, 4423−4432.

BI992187G